第 43 卷 第 20 期/2023 年 10 月/光学学报 研究论文

光学学报

椭圆芯类矩形保偏光纤的设计及其双折射特性

朱玉雪[1]，陈东营[2]，赵强[2,3*]，曲轶[1**]

[1]海南师范大学物理与电子工程学院海南省激光技术与光电功能材料重点实验室，海南 海口 571158；

[2]齐鲁工业大学（山东省科学院）海洋仪器仪表研究所，山东 青岛 266061；

[3]青岛海洋科技中心，山东 青岛 266237

摘要 为了进一步提高传统保偏光纤的双折射，设计了一种高双折射椭圆芯类矩形保偏光纤，该光纤具有一个椭圆芯和两个对称的类矩形应力区。采用数值模拟的方法，全面研究了类矩形应力区的尺寸和纤芯的椭圆度对保偏光纤双折射特性的影响。通过优化参数得到椭圆芯类矩形保偏光纤在1550 nm波长下的双折射为8.0794×10^{-4}，与传统熊猫型保偏光纤的双折射相比增加了近一倍。此外，还研究了所设计光纤在C通信波段（1530～1565 nm）内双折射与波长变化的关系。该光纤结构简单，具有应用于光纤通信和光纤传感领域的潜力。

关键词 保偏光纤；保偏性能；模式双折射；结构优化

中图分类号 TN929.11；TN818；TN253 **文献标志码** A **DOI**：10.3788/AOS231288

1 引 言

保偏光纤具有良好的偏振态保持能力，能抵抗外界干扰，在光纤传感、精密光学仪器、光纤通信等[1-3]领域具有广泛的应用前景。1980年，双折射大小仅为7.35×10^{-5}的保偏光纤已经被应用于温度和压力的同时测量[4]。2005年，Guan等[5]采用有限元法研究了熊猫型、蝶型、椭圆包层型保偏光纤由热应力引起的双折射特性，其中蝶型保偏光纤的双折射高于熊猫型、椭圆包层型保偏光纤的双折射。目前，在高双折射保偏光纤中已经实现光栅的刻写并得到广泛应用[6-7]。光纤的双折射特性会影响光纤传感的应用性能，这使得高双折射保偏光纤成为备受关注的研究对象。

保偏光纤分为形状双折射光纤和应力双折射光纤，研究人员提出了多种双折射光纤，其中形状双折射光纤包括椭圆芯光纤[8-9]、椭圆空芯光纤[10-11]、椭圆环芯光纤[12]、带孔光纤[13-14]等，这类光纤通过改变纤芯形状的不对称性增加光纤的双折射。Corsi等[9]提出的椭圆芯光纤，双折射为1.3×10^{-4}。Hwang等[15]设计的椭圆空芯光纤，在1550 nm处获得2×10^{-4}的双折射，比不含空气孔的光纤的双折射高。应力双折射光纤包括熊猫型保偏光纤[16-17]、蝶型保偏光纤[18-19]、椭圆包层型保偏光纤[20]、类矩形保偏光纤[21]等。Zhang等[22]分析了40 μm直径的椭圆包层型保偏光纤的有限元模型，计算了纤芯处的应力双折射约为10^{-4}。Ren等[21]提出的类矩形保偏光纤，应力诱导的双折射达到了3.98×10^{-4}。目前，这两类光纤的双折射已经达到了10^{-4}的数量级。近年来，为了提高光纤的双折射，人们设计了形状双折射和应力双折射共同作用的高双折射保偏光纤。Song等[23]设计了椭圆环芯的熊猫型保偏光纤，模式双折射为2×10^{-4}。Li等[24]提出了基于叶形芯的熊猫型保偏光纤，模式双折射达到了7.692×10^{-4}，可用于光纤陀螺仪。Zhang等[25]采用三个空气孔辅助椭圆芯蝶型保偏光纤，在1550 nm处模式双折射高达7.76×10^{-4}，具有提高光纤传感器精度的作用。以上设计的高双折射保偏光纤，通过形状双折射和应力双折射的叠加增加了光纤的双折射，能实现光波偏振状态的良好保持，然而，由于制造设备的限制，这类光纤难以在实际中生产。

本文提出了一种形状双折射和应力双折射共同作用的高双折射椭圆芯类矩形保偏光纤，形状双折射依赖于纤芯的椭圆度，而应力双折射依赖于应力区的类矩形结构，具有结构设计简单等优势。仿真研究了类矩形应力区的尺寸、纤芯与应力区的间距、椭圆度对双折射的影响，通过参数优化得到该椭圆芯类矩形保偏光纤的模式双折射可达8.0794×10^{-4}。最后分析了C通信波段（1530～1565 nm）该光纤的双折射特性。结果表明，所提出的光纤具有良好的保偏性能，在光纤通

收稿日期：2023-07-20；**修回日期**：2023-08-23；**录用日期**：2023-09-04；**网络首发日期**：2023-09-14

基金项目：国家自然科学基金（61864002，61933004）、山东省自然科学基金面上资助项目（ZR2020MF108，ZR2022QF086）、博士后资助项目（QDBSH20230102005）、泰山学者工程专项经费资助项目（ts20190951）

通信作者：*zhaoqiang@qlu.edu.cn；**quyihainan@126.com

信和光纤传感领域具有很好的应用前景。

2 保偏光纤双折射理论

保偏光纤的模式双折射主要分为形状双折射和应力双折射，其中形状双折射归因于光纤纤芯几何形状的不对称性，应力双折射是由保偏光纤在制作过程中受到两个正交方向的横向应力不等引起的。

保偏光纤的双折射是衡量保偏光纤偏振特性的关键参数，通常受到纤芯的椭圆度、热膨胀系数等[25]因素的影响。传统圆形芯保偏光纤仅依赖于应力双折射，通过改变纤芯的椭圆度可以在传统圆形芯保偏光纤的基础上改变几何双折射，从而增加保偏光纤的模式双折射。光纤从熔融状态冷却到室温的过程中，由于热应力的产生，可得到纤芯在x、y方向的应力，再利用线性应力-光学效应关系计算x、y方向的折射率。

通常线性应力-光学效应关系[26]可定义为

$$\begin{cases} n_x = n_0 - C_1 S_x - C_2 S_y \\ n_y = n_0 - C_1 S_y - C_2 S_x \end{cases}, \tag{1}$$

式中：$n_i(i=x,y)$表示材料x、y方向分别对应的有效折射率；n_0表示材料无应力时的有效折射率；C_1、C_2表示材料的应力-光学张量；$S_i(i=x,y)$表示材料x、y方向分别对应的应力张量。

应力双折射B_S可定义为

$$B_S = n_x - n_y = (C_2 - C_1)(S_x - S_y)。 \tag{2}$$

模式双折射主要源于形状双折射和应力双折射，其中几何双折射B_G可定义为

$$B_G = e^2 (2\Delta n)^2 f(\nu)/\nu, \tag{3}$$

式中：$e=[1-(a/b)^2]^{1/2}$为椭圆度；a、b分别为纤芯的长半轴和短半轴；ν为光纤的归一化频率；$f(\nu)$为归一化频率的函数。

利用应力-光学效应可得到光纤x、y方向的折射率差值，因此，保偏光纤的模式双折射可定义为

$$B = B_S + B_G = \frac{\beta_x - \beta_y}{k_0} = n_{\mathrm{eff}}^x - n_{\mathrm{eff}}^y, \tag{4}$$

式中：B_S为由于光纤材料的热膨胀系数不同所产生的应力双折射；B_G为由于纤芯几何形状的不对称产生的几何双折射；β_x和β_y表示传播常数；$k_0=2\pi/\lambda$表示波数，其中λ表示真空中的波长；n^x_{eff}、n^y_{eff}分别表示x、y方向上的有效模式折射率。

光纤拉制过程中，由于光纤内部热膨胀系数的差异会在光纤的x、y方向上产生应力差，引起模式双折射。光纤内部的有效折射率与波长和掺杂浓度的关系，可以根据Sellmeier色散公式得到，通过调控纤芯和应力区掺杂的摩尔分数，可以获得掺杂材料的热膨胀系数，表达式[5]为

$$\alpha = (1-m)\alpha_0 + m\alpha_1, \tag{5}$$

式中：α_0和α_1分别表示纤芯和应力区两种掺杂材料的热膨胀系数；$1-m$和m分别表示纤芯和应力区两种掺杂材料的摩尔分数。

3 仿真与分析

3.1 圆形芯类矩形保偏光纤

为了验证所提出的椭圆芯类矩形保偏光纤仿真模型的正确性，首先仿真计算了圆形芯类矩形保偏光纤的双折射，并与现有研究结果进行对比分析[27-28]。如图1所示为圆形芯类矩形保偏光纤的横截面示意图，纤芯半径为a，应力区的长度和宽度分别为j和k，包层半径为r，纤芯与应力区的间距为d。根据光纤材料的有效折射率与掺杂浓度、波长之间的关系，可以通过Sellmeier色散公式计算光纤各个区域的有效折射率，其中纤芯为掺杂GeO_2的SiO_2，有效折射率为1.4558；类矩形的应力区为掺杂B_2O_3的SiO_2，有效折射率为1.4478；包层为纯SiO_2。由式(4)可知，纤芯和包层由于掺杂浓度不同，具有不同的热膨胀系数，光纤从熔融状态冷却到室温，会随温度的变化产生热应变，由于光弹效应产生双折射。设置光纤的纤芯区的热膨胀系数为1.59×10^{-6}，应力区的热膨胀系数为2.215×10^{-6}，包层区的热膨胀系数为5.4×10^{-7}，光纤的熔融温度为1573 K，冷却温度为293 K。

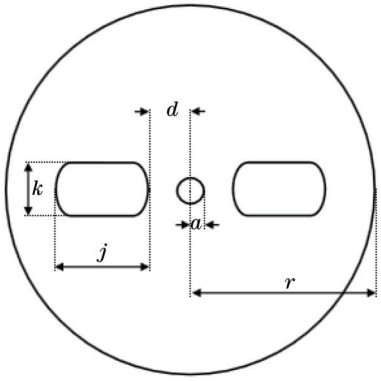

图1 圆形芯类矩形保偏光纤的横截面示意图

Fig. 1 Cross-sectional diagram of circular-core pseudo-rectangle polarization-maintaining fiber

固定纤芯与应力区之间的距离$d=8$ μm，改变应力区长度j(从22 μm增加到30 μm，步长为2 μm)和纤芯半径a(从2.5 μm增加到4.5 μm，步长为0.5 μm)，通过仿真计算得到圆形芯类矩形保偏光纤的模式双折射与应力区长度的函数关系如图2所示。纤芯半径a一定时，增加应力区长度j即增大应力区面积，使应力双折射增加，最终使模式双折射显著增加；应力区长度j一定时，增大纤芯半径a，使模式双折射增加。由此可见，随着纤芯半径a和应力区长度j的增加，模式双折射呈增加趋势。以上得到的仿真结果的变化趋势与文献[27-28]的结果保持一致，验证了模型的正确性。

3.2 椭圆芯类矩形保偏光纤

图3所示为椭圆芯类矩形保偏光纤的横截面示意图，其中应力区的长度和宽度分别为j和k，纤芯与应

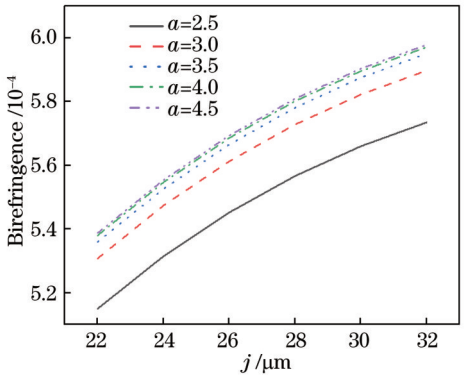

图 2　圆形芯类矩形保偏光纤的模式双折射与应力区长度 j 的函数关系图

Fig. 2　Relationship between mode birefringence and stress zone length j of circular-core pseudo-rectangle polarization-maintaining fiber

力区的间距为 d，纤芯长半轴为 a，短半轴为 b，纤芯的椭圆度定义为 $\rho=a/b$。为了优化纤芯的几何形状得到高双折射，将应力区的长度和宽度分别设置为 $j=24\ \mu m$、$k=14\ \mu m$，纤芯与应力区的间距设置为 $d=8\ \mu m$，改变纤芯的椭圆度 ρ（从 0.5 增加到 0.9，步长为 0.1）和纤芯的长半轴 a（从 3 μm 增加到 5.8 μm，步长为 0.4 μm）。当椭圆度 ρ 小于 1 时，双折射与纤芯短半轴 a 的函数关系如图 4(a)所示。可见，当椭圆度 ρ 一定时，双折射随着纤芯短半轴 a 的增加而降低；当纤芯短半轴 a 一定时，随着椭圆度 ρ 增加，双折射呈增大的趋势。当椭圆度 ρ 从小于 1 变化至大于 1 时，其长、短轴将会改变，双折射与纤芯长半轴 a 的函数关系如图 4(b)所示。随着纤芯长半轴 a 和椭圆度 ρ 的增加，双折射呈增大的趋势。因此，当纤芯的椭圆度 ρ 大于 1 时，随着长半轴 a 的增大，椭圆芯的几何不对称性增加，有效模场面积变大，模场光斑变大，形状双折射增加，从而使得光纤的模式双折射增加。

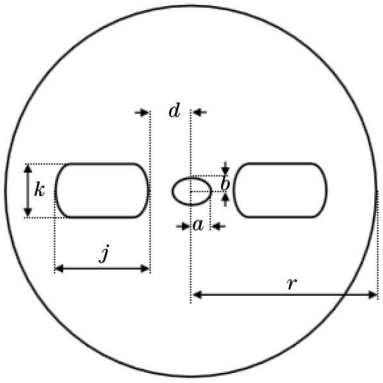

图 3　椭圆芯类矩形保偏光纤的横截面示意图

Fig. 3　Cross-sectional diagram of elliptical-core pseudo-rectangle polarization-maintaining fiber

值得注意的是，与圆形芯类矩形保偏光纤相比，纤芯的椭圆度不同会导致对融的两根光纤产生纤芯失配的现象，对熔接产生一定程度的影响，因此选择合适的椭圆度 ρ 和纤芯长半轴 a 是获得高双折射的关键，也是获取良好偏振性能的先决条件。通过优化后，设置光纤的结构参数，纤芯与应力区的距离 $d=8\ \mu m$，纤芯长半轴 $a=5.8\ \mu m$，当椭圆度 $\rho=1.5$ 时，线性度最好，双折射最大，得到椭圆芯类矩形保偏光纤横截面的 x 方向的冯·米塞斯(von Mises)应力分布图和应力诱导的双折射分布图分别如图 5(a)和 5(b)所示，其双折射达到了 6.534×10^{-4}。

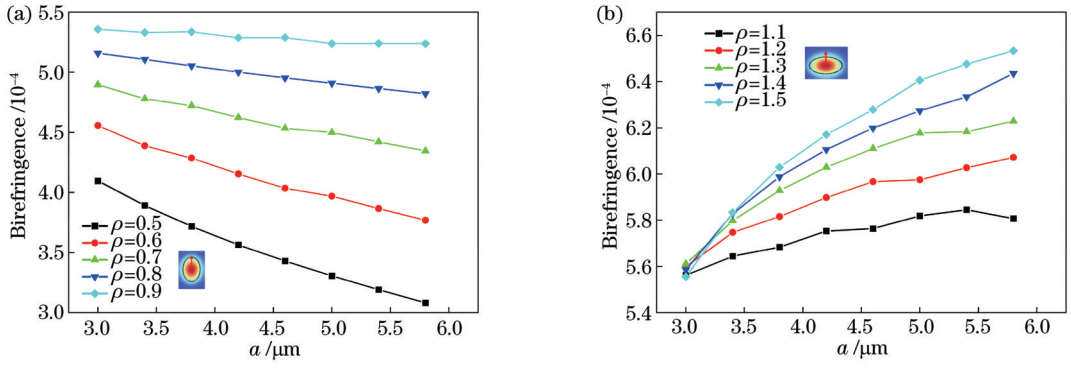

图 4　椭圆芯类矩形保偏光纤的模式双折射的椭圆度与纤芯长半轴 a 的函数关系。(a)纤芯椭圆度 ρ 小于 1；(b)纤芯椭圆度 ρ 大于 1

Fig. 4　Mode birefringent ellipticity of elliptical-core pseudo-rectangle polarization-maintaining fiber as a function of fiber core long half axis a. (a) Core ellipticity ρ is less than 1; (b) core ellipticity ρ is greater than 1

固定椭圆芯和应力区尺寸，改变椭圆芯与应力区的距离 d，得到模式双折射与距离 d 的函数关系如图 6 所示，随着纤芯与应力区之间的距离 d 增加，双折射显著减小。出现这一现象的原因是，d 越小应力区与纤芯的距离越近，使应力引起的双折射增加。在相同距离 d 的条件下，椭圆芯比圆形芯具有更高的双折射，进一步证明了增加纤芯的不对称性可以获得更高的双折射。

为了验证应力区尺寸对双折射的影响，分别研究了应力区的长度 j 和宽度 k 与双折射之间的关系。首先，固定应力区宽度 k 不变，改变应力区长度 j，计算椭圆芯类矩形保偏光纤的模式双折射，得到图 7(a)所示

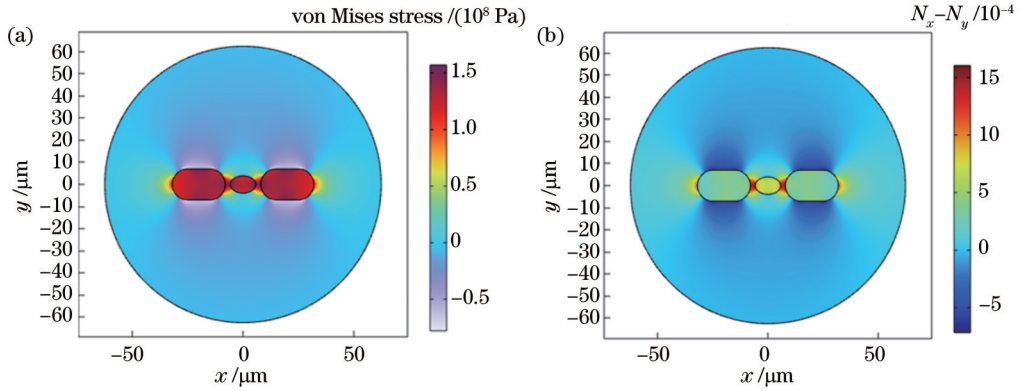

图 5　椭圆芯类矩形保偏光纤横截面。(a)x方向的冯·米塞斯应力分布;(b)应力诱导的双折射分布

Fig. 5　Cross section of elliptical-core pseudo-rectangle polarization-maintaining fiber. (a) von Mises stress distribution in x direction; (b) stress-induced birefringence distribution

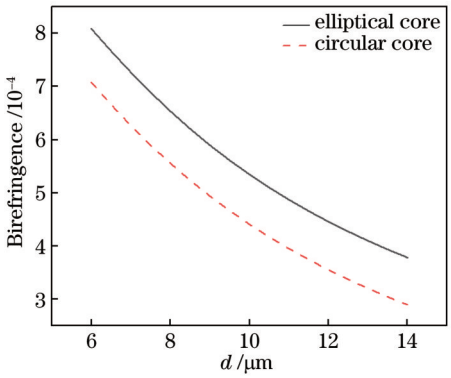

图 6　椭圆芯类矩形保偏光纤与圆形芯类矩形保偏光纤的模式双折射与d的函数关系

Fig. 6　Relationship between mode birefringences and d of elliptical-core pseudo-rectangle polarization-maintaining fiber and circular-core pseudo-rectangle polarization-maintaining fiber

的结果,并与圆形芯类矩形保偏光纤的模式双折射进行对比发现,随着应力区长度j增加,两种类型的保偏光纤的模式双折射均呈现增大的趋势,但双折射相差较大。然后,固定应力区长度j不变,改变应力区宽度k,计算椭圆芯类矩形保偏光纤的模式双折射,得到如图 7(b)所示的结果,并与圆形芯类矩形保偏光纤的模式双折射进行对比发现,随着应力区宽度k增加,两种类型的保偏光纤的模式双折射变化的基本趋势一致,增长速度较快,双折射相差较小。在其他条件不变的情况下,为了获得相同的双折射,椭圆芯类矩形保偏光纤比圆形芯类矩形保偏光纤所需的应力区宽度更小(即应力区面积更小)。因此可以得出,当应力区面积一定时,椭圆芯类矩形保偏光纤具备更高的模式双折射。

利用优化后的椭圆芯类矩形保偏光纤的结构,研究了基模的有效折射率和保偏光纤双折射与波长的依赖关系。光纤基模的有效折射率n_{eff}在C通信波段(1530~1565 nm)的变化曲线如图 8(a)所示,可以看出,基模x、y偏振方向的有效折射率随着波长的增加而减小,当波长大于1565 nm时,基模的y偏振临近截止。图 8(b)为光纤的模式双折射在C通信波段(1530~1565 nm)的变化曲线,可以看出,光纤的模式双折射随波长的增加呈递减的趋势,但变化量相对较小,在波长为1550 nm处,椭圆芯类矩形保偏光纤的模式双折射可达8.0794×10^{-4},与传统熊猫型保偏光纤相比,增加了近一倍[29]。

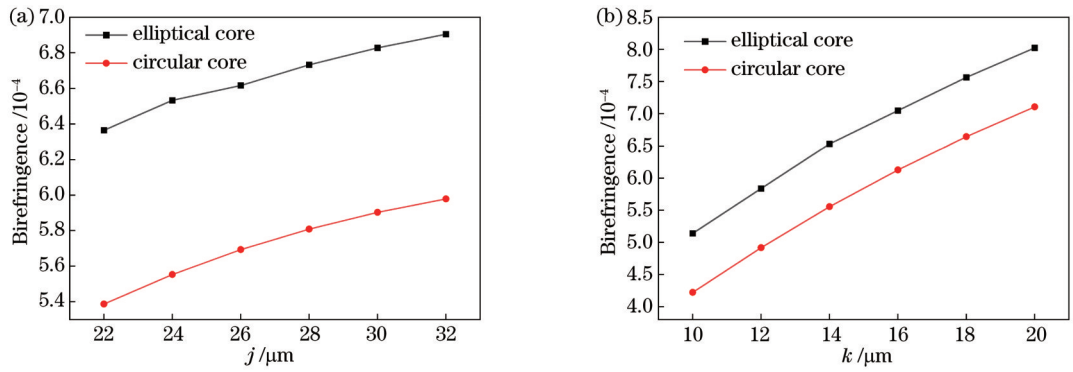

图 7　椭圆芯类矩形保偏光纤和圆形芯类矩形保偏光纤的模式双折射与应力区尺寸的函数关系。(a)应力区长度j;(b)应力区宽度k

Fig. 7　Relationship between mode birefringences and stress zone sizes of elliptical-core pseudo-rectangle polarization-maintaining fiber and circular-core pseudo-rectangle polarization-maintaining fiber. (a) Stress zone length j; (b) stress zone width k

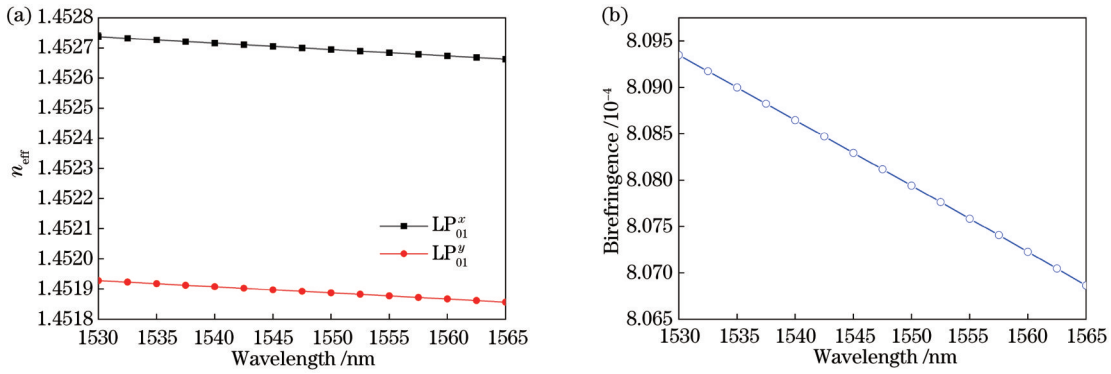

图 8　波长对模式特征的影响。(a)对基模有效折射率的影响;(b)对光纤模式双折射的影响

Fig. 8　Influence of wavelength on mode characteristics. (a) Influence on effective refractive index of fundamental mode; (b) influence on fiber mode birefringence

将本文所设计的光纤与其他文献报道的双折射光纤进行对比如表 1 所示,可以看出,虽然这几种双折射光纤的模式双折射均可达到 10^{-4} 数量级,但本文所设计的光纤的模式双折射明显优于其他光纤,也表明了该光纤具有更好的偏振保持能力,且该光纤具有结构简单、易于制备等优势,有望运用在实际生产中,为开发更高双折射的光纤提供可能。此外,光纤的弯曲损耗是衡量保偏光纤环境适应能力的重要性能参数之一,后续研究中将着重考虑光纤弯曲损耗变化的影响,克服实际工程应用中存在的问题[30]。

表 1　所设计的光纤与其他文献报道的双折射光纤的比较

Table 1　Comparison of proposed fiber with those reported in other references

Reference	Structure	Core type	Central wavelength /nm	Birefringence /10^{-4}
Proposed	Elliptical-core pseudo-rectangle fiber	Elliptical core	1550	8.0794
[24]	Leaf-shape-core panda-type fiber	Leaf-shape core	1550	7.6920
[29]	Circular-core panda-type fiber	Circular core	1550	4.5750
[21]	Elliptical-core fiber with inner cladding	Elliptical core	1550	4.0300
[15]	Fiber with elliptical central air hole	Elliptical central air hole	1550	2.0000
[22]	Elliptical cladding fiber	Circular core	1550	1.2800

4　结　　论

本文提出了一种形状双折射和应力双折射共同作用的椭圆芯类矩形保偏光纤。通过数值模拟的方法,研究了应力区尺寸和纤芯的椭圆度对双折射的影响。研究发现,当椭圆度 ρ 小于 1 时,双折射呈递减的趋势;当椭圆度 ρ 大于 1 时,双折射呈递增的趋势。当椭圆度 $\rho=1.5$ 时,双折射达到了 6.534×10^{-4},因此可以通过增加纤芯几何形状的不对称性改善光纤的双折射。当椭圆度一定时,改变应力区的尺寸也可提高双折射,改变应力区宽度引起的双折射变化比改变应力区长度引起的双折射变化更明显。优化椭圆芯类矩形保偏光纤的结构参数后,在 C 通信波段(1530~1565 nm)范围内,光纤的模式双折射均达到 10^{-4} 数量级以上,当波长为 1550 nm 时,双折射达到了 8.0794×10^{-4},与传统的熊猫型保偏光纤相比,增加了近一倍,能够很好地实现偏振传输。这种保偏光纤在光纤通信和光纤传感领域有巨大的发展潜力。

参　考　文　献

[1]　郭璇, 刘丰, 徐香, 等. 模间干涉的包层腐蚀型椭芯保偏光纤折射率传感特性[J]. 光学学报, 2015, 35(7): 0706002.
Guo X, Liu F, Xu X, et al. Refractive index sensing characteristics of cladding-etched elliptical core polarization maintaining fiber based on intermodal interference[J]. Acta Optica Sinica, 2015, 35(7): 0706002.

[2]　燕苗霞, 李晶, 裴丽, 等. 基于保偏光纤双折射特性的函数波形发生器[J]. 光学学报, 2023, 43(1): 0106001.
Yan M X, Li J, Pei L, et al. Function waveform generator based on birefringence characteristics of polarization maintaining fiber[J]. Acta Optica Sinica, 2023, 43(1): 0106001.

[3]　方莎莎, 吴许强, 张刚, 等. 基于游标效应的高灵敏光纤温度和应变传感器[J]. 中国激光, 2021, 48(1): 0106004.
Fang S S, Wu X Q, Zhang G, et al. High-sensitivity fiber optic temperature and strain sensors based on the vernier effect[J]. Chinese Journal of Lasers, 2021, 48(1): 0106004.

[4]　Eickhoff W. Temperature sensing by mode - mode interference in birefringent optical fibers[J]. Optics Letters, 1981, 6(4): 204-206.

[5]　Guan R F, Zhu F L, Gan Z Y, et al. Stress birefringence analysis of polarization maintaining optical fibers[J]. Optical Fiber Technology, 2005, 11(3): 240-254.

[6]　Liu J, Zhu L Q, He W, et al. Temperature-sensing characteristics of polarization-maintaining fiber Bragg grating inscribed directly by 800-nm femtosecond laser pulses[J]. Optical Fiber Technology, 2020, 56: 102186.

[7]　Zhao Y S, Sun B, Liu Y L, et al. Polarization mode coupling and related effects in fiber Bragg grating inscribed in polarization maintaining fiber[J]. Optics Express, 2016, 24(1): 611-619.

[8] Xiao H, Li H S, Wu B L, et al. Polarization-maintaining terahertz bandgap fiber with a quasi-elliptical hollow-core[J]. Optics & Laser Technology, 2018, 105: 276-280.
[9] Corsi A, Ho Chang J, Wang R H, et al. Highly elliptical core fiber with stress-induced birefringence for mode multiplexing[J]. Optics Letters, 2020, 45(10): 2822-2825.
[10] Zhao J J, Tang M, Oh K, et al. Polarization-maintaining few mode fiber composed of a central circular-hole and an elliptical-ring core[J]. Photonics Research, 2017, 5(3): 261-266.
[11] Xiao H, Li H S, Wu B L, et al. Elliptical hollow-core optical fibers for polarization-maintaining few-mode guidance[J]. Optical Fiber Technology, 2019, 48: 7-11.
[12] Xiao H, Li H S, Jian S S. Hole-assisted polarization-maintaining few-mode fiber[J]. Optics & Laser Technology, 2018, 107: 162-168.
[13] Tan X L, Geng Y F, Zhou J. A novel ultrahigh birefringent hole-assistant microstructured optical fiber with low confinement loss[J]. Optics & Laser Technology, 2011, 43(7): 1331-1334.
[14] Zhu W L, Yi Y T, Yi Z, et al. High confidence plasmonic sensor based on photonic crystal fibers with a U-shaped detection channel[J]. Physical Chemistry Chemical Physics, 2023, 25(12): 8583-8591.
[15] Hwang I K, Lee Y H, Oh K, et al. High birefringence in elliptical hollow optical fiber[J]. Optics Express, 2004, 12(9): 1916-1923.
[16] Jin W, Zhang X, Liu X Q. Highly birefringent one-air-hole panda fiber[J]. Optics Letters, 2023, 48(4): 1004-1007.
[17] 廖世彪, 罗涛, 肖润珩, 等. 国产掺镱保偏光纤的制备及其激光性能研究[J]. 中国激光, 2023, 50(5): 0501002.
Liao S B, Luo T, Xiao R H, et al. Preparation and laser properties of domestic Yb-doped polarization-maintaining fiber [J]. Chinese Journal of Lasers, 2023, 50(5): 0501002.
[18] Zhai C X, Li Y, Wang S S, et al. Study on high sensitivity measurement of seawater temperature based on bow Tie fiber[J]. Optical Fiber Technology, 2023, 76: 103252.
[19] Chen S, Wang J. Fully degeneracy-lifted bow-tie elliptical ring-core multi-mode fiber[J]. Optics Express, 2018, 26(14): 18773-18782.
[20] 关荣锋, 李占涛, 甘志银, 等. 领结型和椭圆型保偏光纤的应力和模式分析[J]. 量子电子学报, 2005, 22(2): 277-281.
Guan R F, Li Z T, Gan Z Y, et al. Analysis on stress and modal field of bow-tie and elliptical cladding polarization-maintaining optical fiber[J]. Chinese Journal of Quantum Electronics, 2005, 22(2): 277-281.
[21] Ren F, Zhangsun T W, Huang X S, et al. Design of 20-polarization-maintaining-mode "pseudo-rectangle" elliptical-core fiber for MIMO-less MDM networks[J]. Optical Fiber Technology, 2019, 50: 87-94.
[22] Zhang T, Liu D Q, Tian S, et al. Birefringence characteristic research of 40 micron supersmall diameter elliptical cladding type polarization maintaining fiber[J]. Proceedings of SPIE, 2014, 9274: 927420.
[23] Song W J, Chen H Y, Wang J P, et al. Panda type elliptical ring core few-mode fiber[J]. Optical Fiber Technology, 2020, 60: 102361.
[24] Li H Y, Li X Y, Zhang Y, et al. Design of high birefringence stress-induced polarization-maintaining fiber based on utilizing geometrical birefringence[J]. Optical Fiber Technology, 2019, 53: 102065.
[25] Li M, Li X Y, Li H Y, et al. Bow-tie holes-aided elliptical-core polarization-maintaining fiber with high birefringence[J]. Optical Fiber Technology, 2022, 73: 103073.
[26] Ji M N, Chen D D, Huang L J. Integration method to calculate the stress field in the optical fiber[J]. Optics Communications, 2017, 403: 103-109.
[27] 文建湘, 苏武, 吴江, 等. 保偏光纤的应力双折射与结构优化[J]. 光纤与电缆及其应用技术, 2008(4): 22-25.
Wen J X, Su W, Wu J, et al. Stress-induced birefringence and structure optimization of PMF[J]. Optical Fiber & Electric Cable and Their Applications, 2008(4): 22-25.
[28] Zheng K, Chang D Y, Fu Y J, et al. Design and fabrication of Panda-type erbium-doped polarization-maintaining fibres[J]. Chinese Physics, 2007, 16(2): 478-484.
[29] 姜暖, 李智忠, 杨华勇, 等. 保偏光纤双折射分析及全光纤拍长测试方法比对研究[J]. 光学学报, 2012, 32(7): 0706003.
Jiang N, Li Z Z, Yang H Y, et al. Birefringence analysis of polarization maintaining fiber and research on characteristic of all-fiber beat-length experimental systems[J]. Acta Optica Sinica, 2012, 32(7): 0706003.
[30] 申文博, 张东生. 弯曲损耗对分布式光纤拉曼测温解调的影响[J]. 激光与光电子学进展, 2023, 60(5): 0506004.
Shen W B, Zhang D S. Influence of bending loss to demodulation on distributed fiber Raman temperature measurement[J]. Laser & Optoelectronics Progress, 2023, 60(5): 0506004.

Design and Birefringence Characteristics of Elliptical-Core Pseudo-Rectangle Polarization-Maintaining Fiber

Zhu Yuxue[1], Chen Dongying[2], Zhao Qiang[2,3*], Qu Yi[1**]

[1]*Hainan Key Laboratory of Laser Technology and Optoelectronic Functional Materials, College of Physics and Electronic Engineering, Hainan Normal University, Haikou* 571158, *Hainan, China*;
[2]*Institute of Oceanographic Instrumentation, Qilu University of Technology (Shandong Academy of Sciences), Qingdao* 266061, *Shandong, China*;
[3]*Qingdao Marine Science and Technology Center, Qingdao* 266237, *Shandong, China*

Abstract

Objective Birefringence is a key parameter to judge whether polarization-maintaining fiber can maintain polarization state, which has research significance. The birefringence of traditional single-mode fibers is very sensitive to subtle changes in the external environment, and two orthogonal polarization modes in fibers are easy to couple. Generally,

polarization-maintaining fibers have strong birefringence, and two orthogonal polarization modes with different propagation constants are not easy to couple. The birefringence caused by external environment changes is far less than that of the fiber itself. Therefore, polarization-maintaining fibers have good polarization-maintaining ability and resistance to external interference, with a wide application prospect in optical fiber sensing, optical components, optical fiber communication, and other fields. We design a high birefringence elliptical-core pseudo-rectangle polarization-maintaining fiber with both shape birefringence and stress birefringence. The shape birefringence depends on the ellipticity of the core, while the stress birefringence depends on the pseudo-rectangle structure in the stress region, which has a simple structural design. The structural parameters are optimized by numerical simulations, and the birefringence of the designed fiber is nearly doubled compared with that of the traditional panda-type polarization-maintaining fiber. The designed high birefringence fiber will be helpful to practical engineering and provide the possibility for the sensing of high birefringence polarization-maintaining fibers.

Methods We study the structure design and birefringence characteristics of numerical simulations in elliptical-core pseudo-rectangle polarization-maintaining fibers. Firstly, the birefringence characteristics of the circular-core pseudo-rectangle polarization-maintaining fiber model are studied and compared with the existing research results to verify the correctness of the proposed polarization-maintaining fiber model. Then, based on the circular-core pseudo-rectangle polarization-maintaining fiber model, the changes in core ellipticity and birefringence characteristics are studied when the core ellipticity changes from less than 1 to more than 1. Then, the von Mises stress distribution and stress-induced birefringence distribution in the x direction of the cross section of the elliptical-core pseudo-rectangle polarization-maintaining fiber are analyzed by simulation software. The influence of the length and width of the stress zone on the birefringence of elliptical-core pseudo-rectangle polarization-maintaining fiber is studied and compared with that of circular-core pseudo-rectangle polarization-maintaining fiber. Next, we research the relationship between the effective refractive index and birefringence of the core fundamental modes in the x and y polarization directions at different wavelengths. Finally, the designed birefringent fibers in other references at home and abroad in recent years are compared.

Results and Discussions When the ellipticity of the designed elliptical core rectangular polarization-maintaining fiber is less than 1, the mode birefringence decreases with the increasing short semi-axis a of the core [Fig. 4(a)]. When the ellipticity of the core is greater than 1, the mode birefringence increases with the rising long semi-axis a of the core [Fig. 4(b)]. The relationship between elliptical-core pseudo-rectangle polarization-maintaining fiber and circular-core pseudo-rectangle polarization-maintaining fiber with the distance between the core and the stress zone is compared and analyzed. As the distance between the core and the stress zone increases, the birefringence decreases significantly (Fig. 5). The functional relationship between the birefringence of elliptical-core pseudo-rectangle polarization-maintaining fiber and circular-core pseudo-rectangle polarization-maintaining fiber is studied respectively. With the increasing length of stress zone, the mode birefringence of the two types of polarization-maintaining fibers tends to rise, but the birefringence is quite different [Fig. 7(a)]. With the increase in the width of the stress zone, the basic trend of the mode birefringence of the two types of polarization-maintaining fibers is the same, with a faster growth rate and smaller birefringence difference [Fig. 7(b)]. Additionally, the birefringence of the designed fiber reaches 8.0794×10^{-4} at the wavelength of 1550 nm [Fig. 8(b)], which is nearly doubled compared with that of the traditional panda-type polarization-maintaining fiber. Thus it has a good polarization-maintaining ability.

Conclusions We design an elliptical-core pseudo-rectangle polarization-maintaining fiber based on shape birefringence and stress birefringence, which has an elliptical core and two symmetric rectangular stress regions. The influence of the size of the rectangular stress region and the core ellipticity on the birefringence of the polarization-maintaining fiber is studied by numerical simulations. When the ellipticity changes from less than 1 to more than 1, the birefringence increases with better polarization-maintaining ability. Under other conditions unchanged, the width of the stress zone required by elliptical-core pseudo-rectangle polarization-maintaining fiber should be smaller than that of circular-core pseudo-rectangle polarization-maintaining fiber to obtain the same birefringence, which indicates a smaller area of stress zone. By optimizing the parameters, the birefringence of elliptical-core pseudo-rectangle polarization-maintaining fiber at 1550 nm is 8.0794×10^{-4}, which is nearly double that of the traditional panda-type polarization-maintaining fiber. Additionally, the relationship between birefringence and wavelength of the proposed fiber in the C communication band (1530–1565 nm) is also studied. The proposed elliptical-core pseudo-rectangle polarization-maintaining fiber has a simple structure and potential applications in optical fiber communication and sensing.

Key words polarization-maintaining fiber; polarization-maintaining performance; mode birefringence; structure optimization